

## Heat capacities and inversions in tridymite, cristobalite, and tridymite-cristobalite mixed phases

ALAN BRUCE THOMPSON AND MECHTHILD WENNEMER

*Institut für Kristallographie und Petrographie  
ETH Zürich, CH-8092, Switzerland*

### Abstract

Samples of synthetic tridymite, cristobalite and tridymite-cristobalite mixed phases, examined by differential scanning calorimetry (DSC) from 360 to 770 or 840K, showed distinct peaks in heat capacity (Cp). For "pure" tridymite the lambda transition at 390K and two peaks near 436K and 470K, which may also be lambda transitions, appear to correlate respectively with the structural changes from (MC) monoclinic (*Cc*) to (OP) orthorhombic  $P2_12_12_1$ , (OP) to (OS) orthorhombic with a non-integral superstructure, and (OS) to (OC) orthorhombic  $C222_1$  described by Nukui *et al.* (1978) as occurring at 383K, 423K, and 463K respectively. It may also be possible to correlate a weak Cp effect near 653K with the (OC) to (HP) hexagonal  $P6_3/mmc$  inversion of Nukui *et al.* The DSC measurements agree with the heat-content measurements by Mosesman and Pitzer (1941) and the dynamic calorimeter data of Shahid and Glasser (1970) for tridymite, although the feature observed in both these studies at 498K was absent in our tridymite sample. This 498K discontinuity probably reflects inversion in cristobalite portions of the "tridymite" samples used in the previous studies, as suggested by our DSC examination of tridymite-cristobalite mixed phases. The present Cp data for tridymite above 500K and for cristobalite above 560K agree reasonably well with the polynomial fits presented by Robie *et al.* (1978, p. 217, 218).

### Introduction

Recent crystallographic studies on tridymite have revealed many more structural modifications than the older work of Gibbs (1927), who identified  $\alpha$ -tridymite as orthorhombic (pseudo-hexagonal) and  $\beta$ -tridymite as hexagonal ( $P6_3/mmc$ ). For example, Dollase (1967) identified, for a tridymite from the Steinbach meteorite, a monoclinic form (twinned pseudo-hexagonal, *Cc* or  $C2/c$ ) at room temperature. Between 380K and 453K Dollase identified a pseudo-hexagonal form similar to high (classical- $\beta$ ) tridymite, with  $a^*$  decreasing from 105Å at 380K to 65Å at 453K, when the satellite reflections faded into background (this type is orthorhombic according to Kihara, 1977). From 453K to above 523K an orthorhombic high tridymite ( $C222_1$ ) exists. Above 523K considerable uncertainty arises from the possibility of cristobalite layers in the tridymite structure (Flörke and Müller-Vonmoos, 1971, p. 200). According to Mischke (1971) the hexagonal (classical- $\beta$ ) form may not exist below about 770K. To complicate matters

further, Konnerth and Appleman (1978) solved the structure of a "terrestrial" low tridymite in a triclinic  $F1$  cell, which they suggest is a lower-temperature form than the "meteoritic" monoclinic form. Many of the apparent structural differences among the X-ray studies probably reflect not only the proportions of tridymite and cristobalite layers in the structure but also their long-range ordering sequences (Flörke, 1967, p. 197).

Nukui *et al.* (1978) studied a synthetic tridymite with X-ray single-crystal and optical methods at elevated temperature, and confirmed the existence of five phases for tridymite. Their MC phase, monoclinic *Cc*, is stable from room temperature to 383K; their OP phase, orthorhombic  $P2_12_12_1$ , is stable between 383 and 423K; their OS phase, orthorhombic with a non-integral superstructure, is stable between 423 and 463K; their OC phase, orthorhombic  $C222_1$ , is stable between 463 and 653K; their HP phase, hexagonal  $P6_3/mmc$ , is stable above 653K. Nukui *et al.* discuss most of the previous crystallographic studies on tridymite and compare the various inversion tem-

peratures (their Fig. 9, p. 1258). Because the inversion characteristics determined by Nukui *et al.* can be most easily correlated with our DSC observations, we have used their nomenclature in our discussion.

Other studies at elevated temperature by dilatometry (Flörke, 1955, p. 378), differential thermal analysis (Flörke, 1955, p. 379; Flörke and Müller-Vonmoos, 1971), and single-crystal studies (Mischke, 1971, p. 20) revealed successive and sometimes continuous changes in structure that may be correlated to large degree with observations made with a microscope heating stage (Fenner, 1913; Flörke, 1955, p. 380; Mischke, 1971; Nukui *et al.*, 1978).

Most of the tridymite inversions have been classified as *displacive* in the classical sense (see Buerger, 1951). This is usually taken to mean that finite discontinuities should be observed for the second-order derivatives of Gibbs energy (*e.g.* heat capacity,  $C_p$ ) at the transition temperature, although many phase transitions so classified in fact exhibit apparently infinite discontinuities in  $C_p$  or occur over a temperature interval and have a latent heat associated with the transition (see Ubbelohde, 1957). It is therefore useful to attempt to correlate the crystallographic aspects of the transformations with any discontinuities in the thermodynamic functions at various temperatures.

The heat capacities of tridymite, cristobalite, and quartz were measured in the range 54K to 295K by Anderson (1936), with an adiabatic calorimeter. In this temperature range the heat capacity of tridymite is virtually identical to those of quartz and cristobalite, and no anomalies were identified in any polymorph. The cristobalite sample used by Anderson (1936, p. 568) was prepared by heating quartz at 1873K for 90 minutes. The conversion to cristobalite was established only by petrographic examination. The tridymite sample used by Anderson was prepared by heating a mixture of 6 parts purified quartz and 1 part  $\text{Na}_2\text{WO}_4$  flux, by weight, at 1523K for 24 hours. It should be noted that tridymite prepared from  $\text{SiO}_2$  gel and  $\text{Na}_2\text{WO}_4$  or  $\text{Na}_2\text{CO}_3$  may show both cristobalite and tridymite reflections in X-ray photographs, depending upon temperature and length of heat treatment (Flörke, 1967, p. 226).

Mosesman and Pitzer (1941) determined the heat content of tridymite from 366.4 to 624.6K. Their samples were from the same material used by Anderson. They observed transitions at 390K and 436K, temperatures close to those observed by X-ray, DTA,

and optical heating methods. They further reported a previously unobserved transition at 498K.

Because Mosesman and Pitzer measured heat content ( $H_T - H_{366.4}$ ) they obtained the heat capacity indirectly by algebraic differentiation. In view of the complex nature of the tridymite inversions and great uncertainties as to their temperatures, because of problems relating to tridymite-cristobalite mixed phases, and also because of similarities with nepheline (Henderson and Thompson, 1980), we decided to examine synthetic samples of tridymite, cristobalite and mixed phases by continuous heating in a differential scanning calorimeter.

After completion of our study, the paper by Shahid and Glasser (1970) was brought to our attention by D. Taylor and C. M. B. Henderson. Shahid and Glasser examined synthetic tridymites prepared with various fluxes, plus one natural sample, with a DuPont dynamic calorimeter and observed  $C_p$ - $T$  behavior very close to that described here, although significantly different in certain aspects.

#### Preparation and characterization of the synthetic material

Pure  $\text{SiO}_2$  gel [MERCK: Kieselgel H (Typ 60:6305111)] was mixed with one mole percent  $\text{K}_2\text{CO}_3$  under acetone in an agate mortar (see Flörke, 1953). The powder was pressed into a pellet, placed on a ceramic tablet, slowly heated to about 1020K, and held there overnight to decompose the carbonate. The sample was heated for 20 hours at 1070K, quenched and reground, then heated for a further 15 hours at 1070K. de Wolff X-ray photographs taken at this stage revealed the presence of both tridymite and cristobalite reflections (sample TR-800 contained about 3/4 tridymite and 1/4 cristobalite). Further heat treatment of this sample for 20 hours at 1170K and then for 20 hours at 2170K produced material exhibiting only tridymite reflections on the de Wolff X-ray photographs (sample TR-G4). However, even sample TR-G4 appears to be still somewhat disordered, from the criteria of Flörke and Langer (1972, p. 224-5).

If instead of  $\text{K}_2\text{CO}_3$ , silica gel is mixed with one mole percent of  $\text{Na}_2\text{CO}_3$  and heat-treated in the same manner as sample TR-G4, material containing about 2/3 cristobalite and 1/3 tridymite (as revealed by de Wolff X-ray photographs) is produced (sample TR-G3).

Samples prepared with pure  $\text{SiO}_2$  gel heated in a platinum envelope at 1770K for 20 hours appeared to

be pure cristobalite on the basis of X-ray photographs (sample CR-1).

Estimation of proportions of phases from the intensity of X-ray powder lines can be very inexact. The proportions of tridymite and cristobalite in these samples were also estimated by comparing their infrared spectra to mechanical mixtures of the two "pure" phases, with the surprising results that TR-800 and TR-G3 appeared to contain about 80 percent and 70 percent of tridymite, respectively.

The cell parameters for the synthetic  $\text{SiO}_2$  phases were determined from measurements of the X-ray powder pattern, obtained with a Guinier-Jagodzinski camera, using the computer program of Visser (1969). From a refinement using 28 lines, cristobalite CR-1 was determined to be tetragonal with  $a = 4.97$  and  $b = 6.92\text{\AA}$ . The refinement for tridymite TR-G4 was less constrained, and for 16 out of 20 lines a monoclinic structure with  $a = 8.22$ ,  $b = 8.60$ ,  $c = 5.01\text{\AA}$  and  $\gamma = 91.5^\circ$  was determined. The refinements for the mixed-layered phases TR-800 and TR-G3 are of course less meaningful and yielded  $a = 12.99$ ,  $b = 10.60$ ,  $c = 12.69\text{\AA}$ ,  $\alpha = 90.5^\circ$  and  $a = 13.32$ ,  $b = 11.03$ ,  $c = 12.25\text{\AA}$ ,  $\gamma = 95.1^\circ$ , respectively, on the basis of 14 out of 20 lines for each.

The samples were analyzed for potassium and sodium by atomic absorption (by B. Ayranci of our institute) and yielded apparent concentrations: TR-G4, 1.29 wt%  $\text{K}_2\text{O}$ , 0.23 wt%  $\text{Na}_2\text{O}$ ; TR-800, 1.38 wt%  $\text{K}_2\text{O}$ , 0.29 wt%  $\text{Na}_2\text{O}$ ; TR-G3, 0.14 wt%  $\text{K}_2\text{O}$ , 1.49 wt%  $\text{Na}_2\text{O}$ . Note that our samples were not washed with acidic solutions prior to DSC examination or atomic absorption analysis. The apparently high concentrations of alkali impurities probably reflect material trapped along grain boundaries, in view of the low concentration levels (50 ppm) reported by Flörke and Langer (1972, p. 223) and Nukui *et al.* (1978, p. 1252) for samples prepared by similar techniques and analyzed after washing in alkaline and acid solutions.

#### Methods and procedures with the differential scanning calorimeter

About 20 mg of powdered  $\text{SiO}_2$  phase was sealed in a preweighed gold pan and the sample placed in the platinum sample holder of the differential scanning calorimeter (a Perkin-Elmer model DSC-2). This sample was run against a preweighed empty gold pan in the matching platinum reference holder from 340 to 600K without cycling the sample through the temperature interval to equalize the lower and upper temperature isothermals (see O'Neill, 1966, for a general discussion of DSC mea-

surement procedures). This scan was followed by a scan of an empty gold pan sample against the same empty gold reference pan as before, over the same temperature interval after isothermal adjustment. This in turn was followed by a scan of a sapphire-standard disc in a gold pan against the same empty gold reference pan as before, over the same temperature interval after isothermal adjustment.

The fourth successive scan was a second heating of the  $\text{SiO}_2$ -phase sample over the same temperature interval, after lower and upper isothermal adjustment. For tridymite TR-G4 the behavior during the second scan was virtually identical to that of the first (unadjusted) scan, except that the first peak (near 395K) became slightly sharper. The very broad displacement between about 420 and 490K was present on both scans. Similar changes of peak intensity were observed during successive heatings of samples TR-G3 and TR-800 (a phenomenon also noticed by Shahid and Glasser, 1970, Fig. 6).

Subsequent heating and cooling scans of the  $\text{SiO}_2$ -phase sample were alternated between scans made on the  $\text{Al}_2\text{O}_3$  standard disc and on high-purity  $\text{Al}_2\text{O}_3$  powder, in gold pans. All scans were made under the same instrument conditions (heating/cooling rate  $10\text{K min}^{-1}$ ; range of  $5\text{ mcal sec}^{-1}\text{ cm}^{-1}$ ; chart speed  $20\text{ mm min}^{-1}$ ; chart range 10 mv). The melting of indium and the  $\alpha$ - $\beta$  quartz inversion were used as temperature and energy calibrations, where the extrapolated onset temperatures were 430K and 844K respectively, with an uncertainty of  $\pm 3\text{K}$ .

#### Evaluation of heat capacity from DSC measurements

The heat capacity of an  $\text{SiO}_2$  phase was evaluated by comparison of the chart displacement for known masses of the  $\text{SiO}_2$  phase and  $\text{Al}_2\text{O}_3$  standard in their respective gold pans, relative to the displacement of the empty gold pan, corrected for deviations of the isothermal baseline and gold pan weights. While the temperature scan is continuous, the heat capacity was evaluated at  $2^\circ$  intervals (Fig. 1). The first  $20^\circ$  of each scan must be regarded as a thermal equilibration interval. The results of several scans over different temperature intervals were used to obtain the heat capacities of the  $\text{SiO}_2$  phases above 360K, as shown in Figures 1, 2, and 3.

#### Correlation of heat capacity data for tridymite, cristobalite and mixed phases with structural transformations

The plot of  $C_p$  ( $\text{J mol}^{-1}\text{K}^{-1}$ ) against temperature (Kelvin) for "pure" tridymite TR-G4 shows several

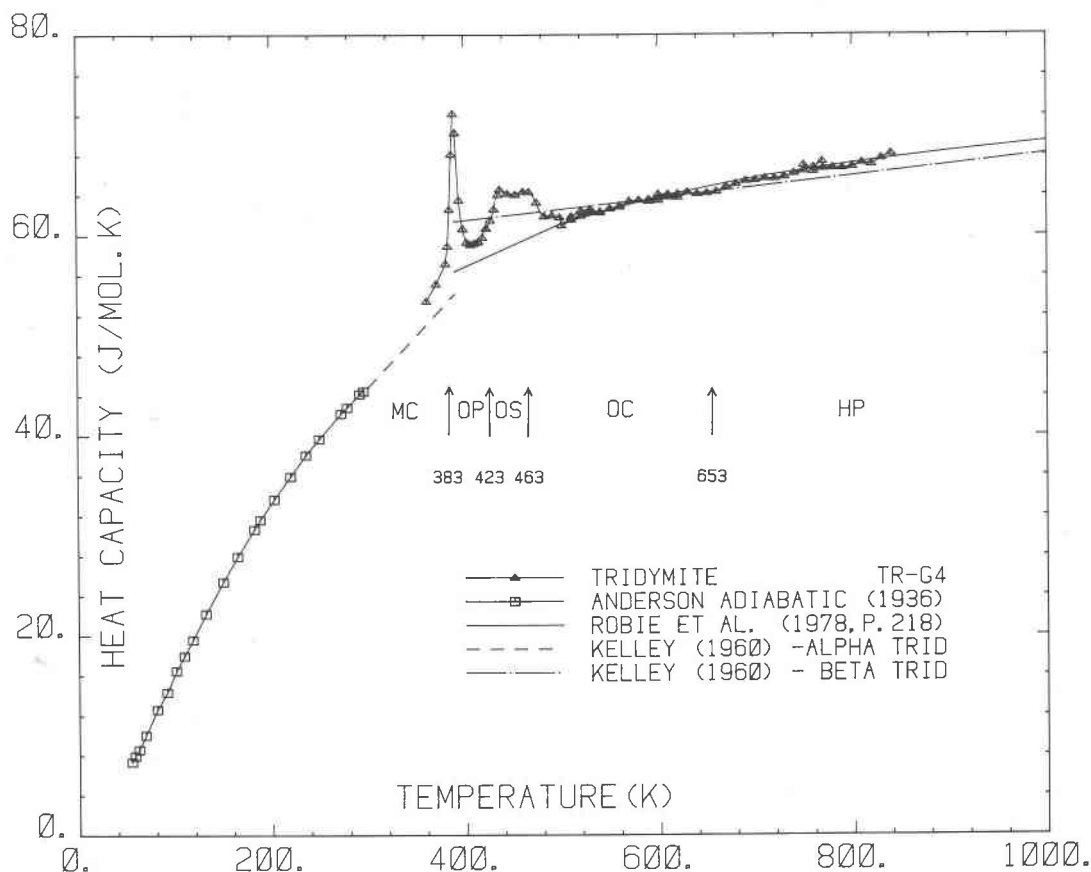


Fig. 1. Heat capacity ( $C_p$  in  $\text{J mol}^{-1}\text{K}^{-1}$ ) against temperature (Kelvin) for the synthetic tridymite (TR-G4) measured by DSC (symbols between 360K and 840K) and from Anderson (1936) measured by adiabatic calorimetry at lower temperatures. Also shown are Kelley's (1960, p. 160) linear fits to the data of Mosesman and Pitzer (1941) for the  $\alpha$  form (298 to 390K), and the  $\beta$  form (390 to 2000K), and the complex polynomial fit for the  $\beta$  form by Robie *et al.* (1978, p. 218). The temperatures indicated by arrows and the correlation with various structural types of Nukui *et al.* (1978, Fig. 9) are discussed in the text.

remarkable features (Fig. 1). The transition at 390K was also observed by Mosesman and Pitzer (1941, Figs. 1 and 4) and by Shahid and Glasser (1970, Figs. 5 and 6) and appears to be a *lambda*-type. The evaluation of the heat of transition is severely complicated by the probable overlap between the first and second peaks. The sharp peak at 390K appears to correlate with a structural change from monoclinic ( $Cc$  or  $C2/c$ , twinned pseudo-hexagonal according to Dollase and Buerger, 1966) to the pseudo-hexagonal form (Dollase, 1967, refined as orthorhombic by Kihara, 1977), or the change from MC to OP as defined by Nukui *et al.* (1978).

The second transition at 436K was also observed by Mosesman and Pitzer and by Shahid and Glasser. Our DSC data indicate that in contrast to the sharpness of the first peak and in contrast to the observation of a relatively narrow second peak by Shahid

and Glasser, the second  $C_p$  peak is broad from 436K to about 470K. Our DSC data also suggest that this broad peak may in fact be two superimposed peaks overlapping near 450K, both of which could be *lambda*-type transitions. If so, these peaks could correspond to the OP-OS inversion and the OS-OC inversion described by Nukui *et al.* (1978) near 423K and 463K respectively. These features are possibly also visible in the measurements of Mosesman and Pitzer (1941, Fig. 1, p. 234a), although they drew a smooth curve through their data between 436 and 498K.

The third transition observed by Mosesman and Pitzer at 498K produced a much more abrupt change in their measured heat content than either of the other transitions. Their observation cannot be reasonably correlated with any significant features in our  $C_p$  measurements, apart from the fact that the

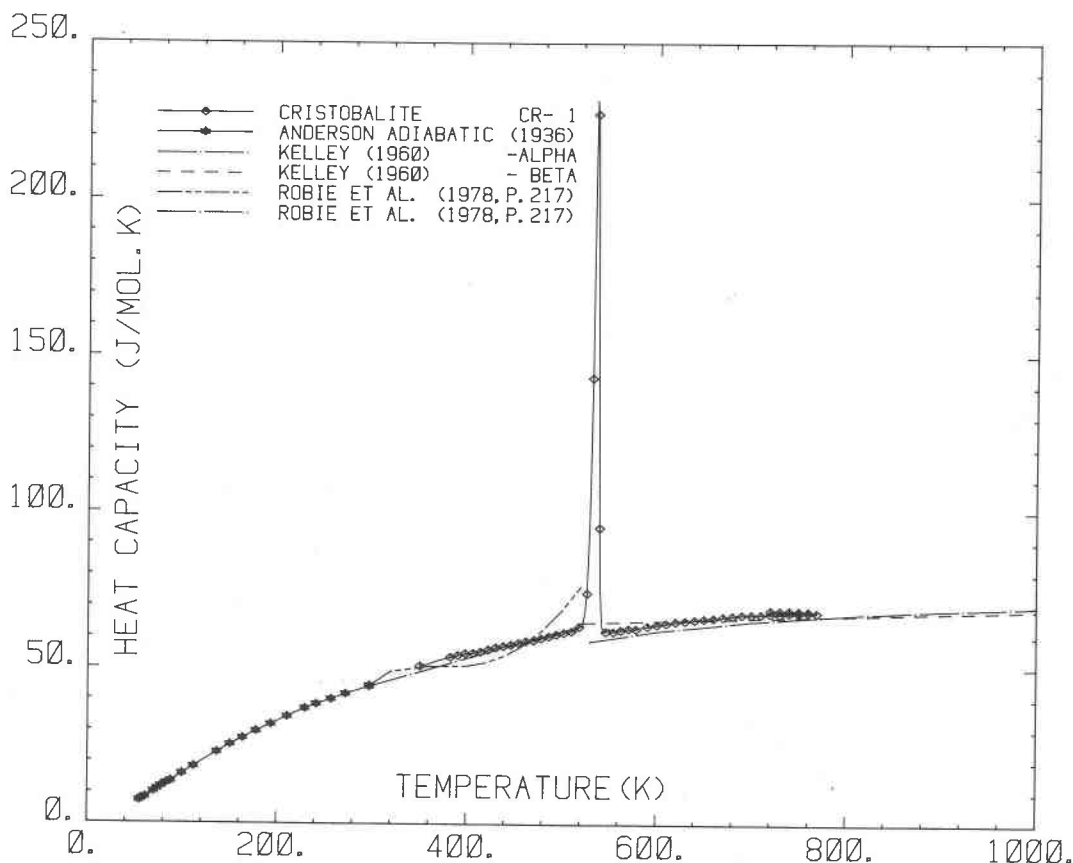


Fig. 2. Heat capacity ( $C_p$  in  $\text{J mol}^{-1}\text{K}^{-1}$ ) against temperature (Kelvin) for the synthetic cristobalite (CR-1) measured by DSC (symbols between 350 and 770K) and from Anderson (1936) measured by adiabatic calorimetry at lower temperatures. Also shown are Kelley's (1960, p. 160) linear fits to the data of Mosesman and Pitzer (1941) for the  $\alpha$  form (298 to 523K) and the  $\beta$  form (523 to 2000K), and the complex polynomial fits for both forms by Robie *et al.* (1978, p. 217).

transitions appear to be complete at this temperature. As no known transition occurs for  $\text{Na}_2\text{WO}_4$  in this region, the discontinuity in heat content is apparently not due to sample impurity. A broad transition near 500K was also observed in some samples examined by Shahid and Glasser (1970, Fig. 5).

Additional problems exist with synthetic tridymite in that cristobalite layers occur in the tridymite structure (Flörke and Müller-Vonmoos, 1971, p. 200) between about 490K and 530K. The apparent discrepancies between our DSC results for tridymite (TR-G4) and the drop calorimetric data of Mosesman and Pitzer prompted the DSC studies of cristobalite and distinct mixed phases.

The sample of synthetic cristobalite (CR-1), was examined using the same DSC instrument settings as those used for tridymite. Figure 2 shows a sharp peak at 535K which marks the "low-high" inversion. Our measurements are in contrast with those of Moses-

man and Pitzer, also on a synthetic cristobalite, who observed a gradual transition interval from about 500K to 540K.

The results of our DSC measurements on the tridymite-cristobalite mixed phases (TR-G3 and TR-800) are shown in Figure 3, compared to our measurements on synthetic tridymite (TR-G4) and cristobalite (CR-1). A crude correlation exists between the proportions of tridymite and cristobalite structures in the samples and the nature of the  $C_p$  vs.  $T$  curves. It may be possible to correlate the diminution and down-temperature displacement of the cristobalite peak with the diminution of the 390K tridymite peak in the sequence from cristobalite (CR-1) through the mixed-phase samples (TR-800 and TR-G3) to tridymite (TR-G4).

Note that sample TR-800 in Figure 3 exhibits the 390K, 436K, and the 498K features of the "tridymite" samples of Mosesman and Pitzer and of Shahid and

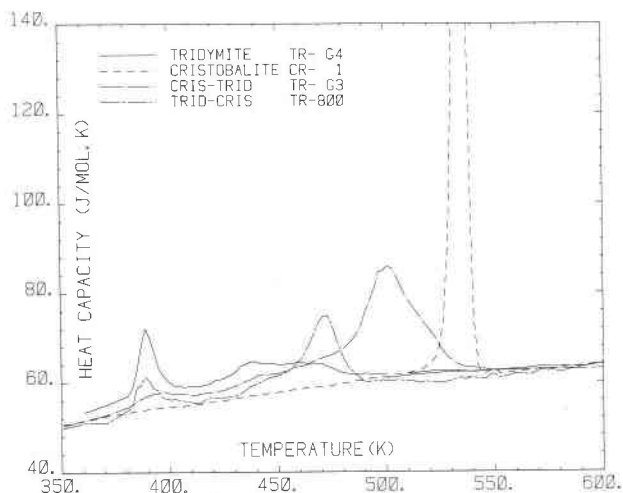


Fig. 3. A comparison of  $C_p$  vs.  $T$  data for two tridymite-cristobalite mixed-phase samples (TR-G3 and TR-800) with data for apparently "pure" tridymite (TR-G4) and cristobalite (CR-1).

Glasser. The abrupt discontinuity at 498K observed by Mosesman and Pitzer (1941, Fig. 1) and the "broad swell" in the range 493K to 523K observed by Shahid and Glasser (1970, Figs. 5 and 6) may represent inversion of cristobalite portions in their "tridymite" samples (see also Flörke, 1967, p. 206).

B. Hemingway (personal communication) noted that the  $C_p$ - $T$  fit (see Fig. 2), obtained by Robie *et al.* (1978, p. 217) from the "low" cristobalite measurements by Mosesman and Pitzer (1941, Fig. 1), bears some similarity to our data for sample TR-G3 (Fig. 3), possibly indicating the presence of "tridymite" layers in the cristobalite sample used by Mosesman and Pitzer.

Nukui *et al.* (1978) described the transition from orthorhombic (OC) to hexagonal (HP) near 653K. It may be possible to correlate this inversion with the slightly lower heat capacities observed near this temperature (see Fig. 1), although this minor displacement is close to the precision limit of the DSC measurements. Flörke (1967, p. 206) notes that DTA and dilatometer studies also show a continuous weak effect between 623K and 733K. Other crystallographic studies (*e.g.* Mischke, 1970, p. 20) suggest that the hexagonal phase does not occur below about 770K.

#### Structural inversions and thermodynamic properties of cristobalite and tridymite

The relatively abrupt transition observed for cristobalite at 535K appears to be of the *first kind*, in

contrast to the lambda transitions observed for tridymite and the mixed phases (and also for quartz) which have been named transitions of the *second kind* by Tisza (1951). Both kinds of transition have associated latent heats and may differ principally in terms of the width of the temperature interval and magnitude of the heat of transition (see Rao and Rao, 1978, p. 17-36).

Our DSC results for cristobalite CR-1, (Fig. 2) show good agreement with an extrapolation of the low-temperature adiabatic data of Anderson (1936) and the  $C_p$  equation fit to various data sources by Kelley (1960, p. 160), *i.e.*

$$C_p(298-523K) = 17.91 + (88.11 \times 10^{-3})T \text{ J mol}^{-1}\text{K}^{-1}$$

It can be seen that poor agreement exists between the above equation, our DSC measurements, and the fit by Robie *et al.* (1978, p. 217) obtained from the heat-content data of Mosesman and Pitzer.

Above the transition, our DSC measurements and the  $C_p$  equation given by Robie *et al.* (1978, p. 217) and by Kelley (1960, p. 160) agree reasonably well, at least above about 600K. The results of our DSC measurements of  $C_p$  for sample CR-1 at various temperatures are presented in Table 1. These data have been smoothed and integrated (using the program HINC, see Robie *et al.*, 1978, p. 2) to give  $H_T-H_{298}$  and  $S_T-S_{298}$  data (Table 2). Using the conventional method of taking areas below the inversion peak relative to extrapolation of the  $C_p$  data to the transition temperature at 535K, a value of about 2320 J mol<sup>-1</sup> results, compared to the value of about 1300 J mol<sup>-1</sup> obtained by Mosesman and Pitzer (1941, p. 2354). The values of  $H_T-H_{298}$  and  $S_T-S_{298}$  are determined by direct integration of the  $C_p$  data for cristobalite CR-1 rather than approximating  $C_p$  to the transition temperature and adding the calculated heat of transition.

Although their heat content measurements did not extend to higher temperatures than 624.5K with precisely calibrated thermocouples, Mosesman and Pitzer (1941, p. 2350) made comparative drops for cristobalite and tridymite samples at 691K, 757K and 818K. They concluded that  $\Delta(H_T-H_{298})$  between cristobalite and tridymite was constant above 548K within their experimental error. Further comparison with cristobalite data was used to obtain the thermodynamic functions for tridymite to 2000K. These data were used by Kelley (1960, p. 160) in his tabulation of thermodynamic data, where he proposed a linear equation

$$C_p = 57.07 + (11.05 \times 10^{-3})T \text{ J mol}^{-1}\text{K}^{-1}$$

Table 1. Measured molar heat capacities of cristobalite (sample CR-1)

TEMP. T KELVIN	HEAT CAPACITY Cp J/(MOL.K)	TEMP. T KELVIN	HEAT CAPACITY Cp J/(MOL.K)
360.76	51.45	536.44	204.73
370.78	52.58	537.44	161.68
380.76	53.31	538.43	127.03
390.74	54.13	539.44	95.07
400.72	54.54	540.43	74.84
410.70	55.04	542.43	63.41
420.68	55.65	546.42	61.88
430.66	56.67	550.41	62.93
440.64	57.22	560.41	62.43
450.62	57.88	570.37	62.84
460.60	58.53	580.35	63.16
470.58	59.03	600.31	64.21
480.55	59.91	610.29	64.57
490.53	60.58	620.26	65.11
500.51	60.99	630.24	65.41
510.49	62.01	640.22	65.73
520.47	64.18	650.20	66.09
522.47	65.22	660.18	66.32
524.46	67.90	670.16	66.70
526.46	74.19	680.14	67.04
528.46	90.11	690.12	67.42
529.45	102.22	700.10	67.46
530.45	122.08	710.08	67.53
531.45	143.04	720.06	67.74
532.45	178.08	730.04	67.59
533.44	207.56	740.02	67.94
534.44	231.73	750.00	67.92
535.44	227.29	759.97	68.18

Temperatures were calibrated against a slope-onset for the melting of Indium at 429.7K and the  $\alpha$ - $\beta$  Quartz inversion at 844K. Uncertainty  $\pm 3$ K. A gram formula weight of 60.085 was used. Heat capacity determined with reference to the values for  $\alpha$ -Al<sub>2</sub>O<sub>3</sub> reported by Dittmars and Douglas (1971). Values of Cp at two-degree intervals above and below the transition were measured and are available from the authors on request. On the basis of alternate scans on Al<sub>2</sub>O<sub>3</sub> the data are believed to be accurate to within one percent.

for  $\beta$ -tridymite from 390 to 2000K. This equation is also plotted in Figure 1 and does not reproduce the present Cp values very accurately, even those above 500K. Robie *et al.* (1978, p. 218) refitted the heat content data of Mosesman and Pitzer to obtain the relation

$$C_p = 74.904 + 3.099 \times 10^{-3}T - 2.3669 \times 10^{-2}T^{-0.5} - 1.17 \times 10^6 T^{-2} \text{ J mol}^{-1}\text{K}^{-1}$$

While Robie *et al.* (1978, p. 218), following Kelley, suggested their equation is valid from 390 to 1800K, it only reproduces the present measurements above 500K reasonably well, apart from the low region in the range 620 to 700K which may be correlated with

the OC-HP transition described by Nukui *et al.* (1978) at 653K.

Kelley (1960, p. 160) presented a linear fit to the graph of Mosesman and Pitzer (1941) between 298 and 390K which he considered to represent  $\alpha$ -tridymite

$$C_p = 13.68 + (103.76 \times 10^{-3})T \text{ J mol}^{-1}\text{K}^{-1}$$

This line is also shown in Figure 1 and coincides with the upper temperature range of the heat capacity measurements made by Anderson (1936).

Table 3 gives our Cp measurements for tridymite TR-G4 at various temperatures above 360K. Our measurements (Fig. 1) show an offset towards higher values of Cp than the Kelley (1960, p. 160) equation for  $\alpha$ -tridymite and an extrapolation of the Anderson (1936) low-temperature adiabatic data. Comparison of heat capacity of the sapphire standard disc or

Table 2. Molar thermodynamic properties for cristobalite CR-1

T KELVIN	Cp J/(MOL.K)	H <sub>T</sub> -H <sub>T</sub> <sup>298</sup> J/(MOL)	S <sub>T</sub> -S <sub>T</sub> <sup>298</sup> J/(MOL.K)
298.15	45.18	0	0
300.00	45.40	83.8	0.28
350.00	50.45	2485.9	7.68
400.00	54.45	5111.3	14.68
450.00	57.92	7922.2	21.30
500.00	61.12	10899.1	27.57
510.00	61.74	11513.5	28.79
520.00	64.16	12006.0	29.75
526.00	71.42	12394.5	30.49
530.00	115.58	12752.5	31.16
534.00	220.87	13400.6	32.38
536.00	212.59	13910.7	34.48
540.00	85.57	14485.5	35.55
542.00	61.13	14625.8	35.81
550.00	61.43	15096.4	36.67
560.00	62.08	15714.0	37.78
570.00	62.67	16337.8	38.89
580.00	63.23	16967.4	39.98
590.00	63.74	17602.2	41.07
600.00	64.21	18242.0	42.14
650.00	66.08	21502.5	47.36
700.00	67.29	24839.3	52.31
750.00	68.02	28223.9	56.98

Smoothed values were obtained from the measured Cp data in Table 1 by polynomial fits over temperature segments. Note that the integrated functions have not been adjusted for heat or entropy of transition at 535K.

The smoothed Cp equations used outside the transition interval are Cp(298-510K) = 82.00 + 0.11397T - 1.30784x10<sup>6</sup>T<sup>-2</sup> - 3.2482T<sup>-0.5</sup> Cp(556-770K) = 101.4996 - 0.02627T - 7.74839x10<sup>6</sup>T<sup>-2</sup>.

$\text{Al}_2\text{O}_3$  powder, obtained on alternate scans with tridymite TR-G4, indicate a deviation of less than 1 percent relative to the  $C_p$  data for  $\alpha\text{-Al}_2\text{O}_3$  of Dittmars and Douglas (1971). It is not known if this offset could conceal the transition at 337K described by Sosman (1965, p. 95). We plan to investigate the temperature interval from 100 to 390 K for these and other samples of tridymite with the low-temperature attachment for the differential scanning calorimeter, and include our low-temperature data before presenting thermodynamic functions for tridymite.

Despite the significant differences observed in  $C_p$  behavior as a function of temperature in the vicinity of the transitions, tridymite, cristobalite, and presumably also the mixed phases exhibit virtually identical heat capacities at lower and higher temperatures than in the range of the transitions.

#### Further investigations of tridymite-cristobalite inversions

Clearly the nature of the flux used in synthesis and the sample history have noticeable effects on the inversion nature of tridymite-cristobalite samples. Although the results presented in Figure 3 indicate that the "mixed phases" are structural interlayers of tridymite and cristobalite, the tridymite portions may be stabilized by synthesis impurities and thus represent temporary modifications rather than permanent features of the crystal structure. In this regard it should be mentioned that peak intensity on the DSC is substantially modified by consecutive scans through the temperature intervals of the tridymite inversions (see also Shahid and Glasser, 1970). We plan to investigate further (with the DSC from 100K upwards) tridymite and cristobalite samples prepared by various methods and under different heat treatments to ascertain the amount of impurities incorporated in the lattice, the nature of the mixed phases, and the effect of sample history on the magnitude of the inversions.

Most of the inversions between the various tridymite and cristobalite structures appear to involve a heat of transition, even those which exhibit broad (and in some cases may be referred to as order-disorder transitions) rather than sharp features. The "classical methods" of evaluation of heats of transition and other thermodynamic functions from drop calorimetry usually made  $50^\circ$  or  $100^\circ$  apart (see Kelley, 1960, p. 2-9) cannot distinguish transitions with small energies from normal scatter in the data, or further characterize the structural changes observed in

Table 3. Measured molar heat capacities of tridymite (sample TR-G4)

TEMP.	HEAT CAPACITY	TEMP.	HEAT CAPACITY
T KELVIN	$C_p$ J/(MOL.K)	T KELVIN	$C_p$ J/(MOL.K)
360.80	53.39	474.57	63.24
370.78	55.09	476.56	62.79
380.76	57.13	478.56	62.29
382.76	58.88	480.55	62.13
384.75	62.54	482.55	61.85
386.75	68.06	484.55	61.87
388.75	72.13	486.54	61.90
390.74	70.22	488.54	61.87
392.74	67.05	490.53	61.94
394.73	63.46	492.53	61.82
396.73	61.84	494.53	61.84
398.72	60.61	496.52	61.86
400.72	59.81	498.52	61.74
402.72	59.27	500.51	61.72
404.71	59.29	510.49	61.84
406.71	59.03	520.24	61.89
408.70	59.15	530.22	62.26
410.70	59.18	540.21	62.32
412.70	59.06	550.41	62.61
414.69	59.32	560.39	62.89
416.69	59.53	570.17	63.37
418.68	59.74	580.16	63.44
420.67	60.53	590.14	63.34
422.67	60.65	600.13	64.06
424.67	60.86	610.12	64.05
426.66	61.45	620.10	64.07
428.66	61.80	630.24	64.25
430.66	62.54	640.22	64.08
432.65	63.66	650.20	64.15
434.65	64.01	660.18	64.27
436.65	64.57	670.16	64.78
438.64	64.75	680.14	65.02
440.64	64.41	690.12	65.34
442.63	64.28	700.10	65.40
444.63	64.12	710.08	65.60
446.63	64.17	720.06	65.56
448.62	64.17	730.04	65.75
450.62	63.83	740.02	66.09
452.61	64.02	750.00	66.34
454.61	64.21	759.97	66.67
456.60	64.21	769.90	66.58
458.60	64.49	779.89	66.64
460.60	64.34	789.87	66.62
462.59	64.33	799.86	66.75
464.59	64.23	809.85	67.16
466.58	64.31	819.83	66.99
468.58	64.16	829.82	67.59
470.58	64.09	839.81	68.04
472.57.	63.55		

See Footnotes to Table 1.

recent X-ray studies. The continuous evaluation of heat capacity as a function of temperature obtained by differential scanning calorimetry, when combined with structural data, provides a much better evaluation of the nature, heat and temperature intervals of transition than most drop calorimetric studies performed on minerals.

### Acknowledgments

We thank G. Bayer, O. W. Flörke, and especially B. Hemingway for extremely helpful discussions. The DSC is supported by E.T.H. Special Project Funds.

### References

- Anderson, C. T. (1936) The heat capacities of quartz, cristobalite and tridymite at low temperatures. *J. Am. Chem. Soc.*, **58**, 568–570.
- Buerger, M. J. (1951) Crystallographic aspects of phase transformations. In R. Smoluchowski, J. E. Mayer and W. A. Weyl, Eds., *Phase Transformations in Solids*, p. 183–211. Wiley, New York.
- Ditmars, D. A. and T. B. Douglas (1971) Measurement of the relative enthalpy of pure  $\alpha$ - $\text{Al}_2\text{O}_3$  (NBS Heat capacity and enthalpy standard reference material No. 720) from 273 to 1173K. *J. Res. Natl. Bur. Stand.*, **75A**, 401–420.
- Dollase, W. A. (1967) The crystal structure at 220°C of orthorhombic high tridymite from the Steinbach meteorite. *Acta Crystallogr.* **23**, 617–623.
- and M. J. Buerger (1966) Crystal structure of some meteoritic tridymites (abstr.). *Geol. Soc. Am. Program 1966 Annual Meeting*, 54–55.
- Fenner, C. N. (1913) The stability relations of the silica minerals. *Am. J. Sci.*, **36**, 331–384.
- Flörke, O. W. (1953) Der Einfluss der Alkali-Ionen auf die Kristallisation des  $\text{SiO}_2$ . *Fortschr. Mineral.*, **32**, 33–35.
- (1955) Strukturanomalien bei Tridymit und Cristobalit. *Ber. Deutsch. Keram. Ges.*, **32**, 369–381.
- (1967) Die Modifikationen von  $\text{SiO}_2$ . *Fortschr. Mineral.*, **44**, 181–230.
- and K. Langer (1972) Hydrothermal recrystallisation and transformation of tridymite. *Contrib. Mineral. Petrol.*, **36**, 221–230.
- and M. Müller-Vonmoos (1971) Displazive Tief-Hoch-Umwandlung von Tridymit. *Z. Kristallogr.*, **133**, 193–202.
- Gibbs, R. E. (1927) The polymorphism of silicon dioxide and the structure of tridymite. *Proc. R. Soc. Lond.*, **A113**, 351–368.
- Henderson, C. M. B. and A. B. Thompson (1980) An investigation of the low-temperature inversion in nepheline using differential scanning calorimetry. *Am. Mineral.*, in press.
- Kelley, K. K. (1960) Contributions to the data on theoretical metallurgy XIII: high-temperature heat-content, heat-capacity, and entropy data for the elements and inorganic compounds. *U.S. Bur. Mines Bull.* **584**.
- Kihara, K. (1977) An orthorhombic superstructure of tridymite existing between about 105 and 180°C. *Z. Kristallogr.*, **146**, 185–203.
- Konnert, J. H. and D. E. Appleman (1978) The crystal structure of low tridymite. *Acta Crystallogr.*, **B34**, 391–403.
- Mischke, H. (1971) *Die Sauerstoffbrücken in der Kristallstruktur des Tridymites bei 500°C*. Diplomarbeit, Westfälische Wilhelms Universität, Münster.
- Mosesman, M. A. and K. S. Pitzer (1941) Thermodynamic properties of the crystalline forms of silica. *J. Am. Chem. Soc.*, **63**, 2348–2356.
- Nukui, A., H. Nakazawa and M. Akao (1978) Thermal changes in monoclinic tridymite. *Am. Mineral.*, **63**, 1252–1259.
- O'Neill, M. J. (1966) Measurement of specific heat functions by differential scanning calorimetry. *Anal. Chem.*, **38**, 1331–1336.
- Rao, C. N. R. and K. J. Rao (1978) *Phase Transitions in Solids*. McGraw-Hill, New York.
- Robie, R. A., B. S. Hemingway and J. R. Fisher (1978) Thermodynamic properties of minerals and related substances at 298.15K and one bar ( $10^5$  pascals) pressure and at higher temperatures. *U.S. Geol. Surv. Bull.* **1452**.
- Shahid, K. A. and F. P. Glasser (1970) Thermal properties of tridymite: 25°C–300°C. *J. Thermal Analysis*, **2**, 181–190.
- Sosman, R. B. (1965) *The Phases of Silica*. Rutgers University Press, New Jersey.
- Tisza, L. (1951) On the general theory of phase transitions. In R. Smoluchowski, J. E. Mayer and W. A. Weyl, Eds., *Phase Transformations in Solids*, p. 1–37. Wiley, New York.
- Ubbelohde, A. R. (1957) Thermal transformations in solids. *Chem. Soc. Lond. Quart. Rev.*, **11**, 246–272.
- Visser, J. W. (1969) A fully automatic program for finding the unit cell from powder data. *J. Appl. Crystallogr.*, **2**, 89.

Manuscript received, December 11, 1978;  
accepted for publication, May 11, 1979.